



## Short Communication

## Alloy design and property evaluation of new Ti–Cr–Nb alloys

Ljerka Slokar\*, Tanja Matković, Prosper Matković

University of Zagreb, Faculty of Metallurgy, Department of Physical Metallurgy, Aleja narodnih heroja 3, 44103 Sisak, Croatia

## ARTICLE INFO

## Article history:

Received 10 May 2011

Accepted 22 June 2011

Available online 13 July 2011

## ABSTRACT

Titanium and its alloys are extensively used as biomedical implant materials because their good mechanical properties are accompanied by an excellent biocompatibility and corrosion resistance. However, the most widely used Ti alloy for medical implants, Ti–6Al–4V, does not satisfy a major requirements about non-toxicity and low elastic modulus close to that of cortical bone. Therefore, alternative titanium-based biomedical alloys with other alloying elements are currently the subject of intensive study.

This work was conducted to develop new as-cast Ti-based alloys with biocompatible elements, i.e. chromium and niobium addition and low elastic modulus. For this purpose six Ti–Cr–Nb alloys were prepared and their properties were evaluated. The obtained results indicated that experimental alloys have  $\alpha/\beta$  microstructure. Among them, alloys  $Ti_{70}Cr_{10}Nb_{20}$ ,  $Ti_{70}Cr_{20}Nb_{10}$  and  $Ti_{60}Cr_{20}Nb_{20}$  have very low elastic modulus (17–50 GPa), high strength (1580–1700 MPa) and plasticity (75.0–83.5%) as well as an excellent corrosion resistance. According to the obtained results it could be considered that new biomedical alloys with adequate properties for biomedical applications were developed.

© 2011 Elsevier Ltd. All rights reserved.

## 1. Introduction

Nowadays, considerable efforts have been devoted by materials scientists and engineers to the development of new materials for biomedical applications with low elastic modulus and superior biocompatibility. Some of the widely used biomaterials (stainless steels, Co–Cr alloys, Ti–6Al–4V) can potentially cause some health problems. Namely, besides the release of toxic metal ions, they can also lead to resorption of adjacent bone tissue due to the great difference in elastic modulus between the implant and human bone [1]. Among the metallic materials, titanium alloys exhibit the lowest elastic modulus (100–110 GPa), but it is still significantly higher than that of bone tissue (10–40 GPa) [2]. However, titanium and its alloys possess good mechanical properties, such as high strength, relatively low elastic modulus and good corrosion resistance, as well as biocompatibility [3,4].

In this paper the microstructure, mechanical properties and corrosion behavior of ternary Ti–Cr–Nb alloys were investigated. Chromium and niobium were selected as  $\beta$ -phase improving and  $\beta$ -phase forming elements, respectively. Namely, titanium alloys of  $\beta$ -type exhibit lower elastic modulus than Ti-alloys of  $\alpha$ -type [5,6]. Furthermore, chromium reduces the high melting temperature of pure titanium and it is known to control the anodic activity and increase the tendency of titanium to passivate. Tissue reaction studies have identified niobium as non-toxic element, as it does not cause any adverse reaction in human body. Also, niobium is

$\beta$ -stabilizer and it forms homogenous solid solution with titanium [7–9].

## 2. Experimental procedure

A six Ti–Cr–Nb alloys with 60–80 atomic percent (at.%) of titanium and 10–30 at.% of niobium, the balance was chromium, were developed. They were prepared by melting a high purity elements (>99.9%) in a water-cooled copper crucible using a tungsten electrode arc in a vacuum chamber purged with argon. Because of a large difference in the melting temperature of pure elements, samples were prepared in two steps. First, the ingots made from chromium and niobium were re-melted a three times and then titanium was added. These button-like ingots were melted by turning them upside down a four times to ensure chemical and structural homogeneity. The casting was realized in the same equipment by means of specially constructed copper anode, which served also as a casting mold. In this way, as cast cylindrical samples with dimensions  $8 \times 25$  mm were obtained. They were sectioned using a Buehler Isomet low-speed diamond saw to attain a several samples for different examinations.

The samples for optical observation were prepared by a standard metallographic procedure which consists of grinding up to 1200 grit with SiC, polishing with 0.05  $\mu$ m alumina powder to mirror finish and distilled water washing. The microstructure was clearly visible, so there was no need for etching. Microstructural observations were then performed using a scanning electron microscope (SEM) Tescan Vega TS 5136 MM with technique of back-scattered electrons (BSE) and energy dispersive X-ray (EDX) analyzer of Bruker type.

\* Corresponding author. Tel.: +385 44 533 381; fax: +385 44 533 378.

E-mail address: [slokar@simet.hr](mailto:slokar@simet.hr) (L. Slokar).

In order to verify the phase constitution in as-cast alloys X-ray diffraction (XRD) measurements were carried out on polished discs surfaces. XRD patterns were obtained utilizing a Philips PW 3710 diffractometer operated at 40 kV and 40 mA with Cu K $\alpha$  radiation and a wavelength of 0.15406 nm. The phases were identified by matching each characteristic peak with JCPDS files [10]. The lattice parameters of phases present in as-cast specimens were calculated using computer program CELREF. This program refines cell parameters from powder diffraction data. First step in refinement is to search for the most probable assignment of Millers indices to powder diffractograms starting from approximate unit cell parameters. In our calculation we have used cell parameters of pure  $\beta$ - and  $\alpha$ -titanium. Once an angle-dispersive powder diffraction pattern for investigated (substitutional) alloys has been indexed, it may be reduced to a list of  $hkl$  and observed  $2\theta$  value. Now unit cell constants may be refined by least-squares fitting procedure that minimizes the quantity (by changing initial cell parameters by small increments or decrements):

$$\sum_{n=1}^N wn\{2\theta n(\text{obs}) - 2\theta n(\text{calc})\}^2 \quad (1)$$

where

$$2\theta n(\text{calc}) = 2 \sin^{-1}(\lambda/2d) \\ = 2 \sin^{-1} \left\{ \lambda \sqrt{(Ah^2 + Bk^2 + Cl^2 + Dhl + Ekl + Fhk)/2} \right\} \quad (2)$$

(A–F values refer to cell parameters). The weighting factor of observed reflections,  $w$ , equals the reciprocal of the variance of the observation  $\sigma^2$  and, the refinement should take in the account constraints due to the symmetry of the crystal system [11].

Mechanical characterization of as-cast Ti–Cr–Nb alloys was based on hardness and compressive tests. Hardness measurements were performed by Vickers method (20 N, 10 s) on the Mitutoyo HV 112–114 testing machine. Compressive tests were carried out on the as-cast circular specimens with dimensions  $8 \times 10$  mm in a Amsler testing machine at strain rate of  $1 \times 10^{-4}$ /s at a room temperature. From the stress–compression curves elastic moduli, compressive and yield strength as well as plastic strain were determined [12–14].

The corrosion resistance of experimental alloys was evaluated on the basis of pitting potential  $E_{\text{pitt}}$ , i.e. the potential of the passive film breakdown. Measurements were carried out by the method of cyclic potentiodynamic anodic polarization at a scanning rate of 5 mV/s between –1000 and +3000 mV in aerated 0.9% NaCl aqueous solution at the temperature of 37 °C on the equipment Ametek type Parstat 2273. The working electrodes consist of Ti–Cr–Nb alloys samples grinded up to 600 grit with SiC and placed at the glass corrosion cell kit, leaving a circular 50 mm<sup>2</sup> metal surface in contact with electrolyte.

### 3. Results and discussion

#### 3.1. Microstructures and XRD analysis

Microstructural observations of experimental alloys performed by SEM with BSE technique showed that all of them have a two-phases microstructure (Fig. 1a–f). It consists of dendritic and interdendritic regions, which can be seen on the microphotographs as dark and light areas. In the microstructure of alloys Ti<sub>60</sub>Cr<sub>10</sub>Nb<sub>30</sub>, Ti<sub>60</sub>Cr<sub>20</sub>Nb<sub>20</sub> and Ti<sub>60</sub>Cr<sub>30</sub>Nb<sub>10</sub> a presence of third needle-like phase was observed. Fig. 2 shows XRD profiles for all experimental alloys. The squares in the figure indicate peaks due to the body-centered cubic (bcc)-structured  $\beta$  phase and the triangles indicate peaks

from the hexagonal (hcp)  $\alpha$  phase. The results of XRD analysis showed that all experimental alloys were two-phases alloys. Diffraction pattern of Ti<sub>80</sub>Cr<sub>10</sub>Nb<sub>10</sub> alloy indicated strong peaks for  $\beta$  phase with bcc lattice and weaker peaks for  $\alpha$  phase with hcp lattice. Other diffraction patterns were very similar and indicated the peaks for  $\beta$  and  $\alpha$  phase with closely intensity. Hence, XRD analysis showed that all experimental as-cast Ti–Cr–Nb alloys consist of  $\beta$  and  $\alpha$  phase, what is in a good agreement with the results for Ti–Nb alloys with silicon, molybdenum and tin as  $\beta$ -stabilizers [6,15,16]. According to the diffraction peaks intensity and diffraction angles, the interdendritic region on the microphotographs (Fig. 1a–f) was identified as the  $\beta$  phase, while the dendrites were identified as the  $\alpha$  phase. A needle-like feature was not registered in XRD patterns, probably because of its small amount in the microstructure. However, according to the literature data for Ti–Nb based biomedical alloys [17,18] and its characteristic form, appearance of needles in the microstructure, is the proof for martensitic transformation of  $\beta$  to  $\alpha'$  phase.

The values of the lattice parameters for  $\beta$  and  $\alpha$  phase (Table 1) were calculated using the Celref program. Results show that the lattice parameters were reduced concerning those for the pure  $\beta$ -Ti ( $a = 0.331$  nm) and  $\alpha$ -Ti ( $a = 0.295$  nm,  $c = 0.468$  nm), respectively. Since the atomic radius of substitutional alloying elements, i.e. chromium (0.130 nm) and niobium (0.145 nm) were smaller than that for titanium (0.147 nm), the original lattice parameters of  $\beta$ - and  $\alpha$ -Ti were reduced through the formation of the  $\beta$ - and  $\alpha$ -Ti solid solutions, respectively. Further, the lattice parameter of  $\beta$  phase is reduced with increasing chromium content (10 up to 30 at.%), as an alloying element with the smaller atomic radius.

In order to obtain the average chemical composition of phases presented in experimental alloys, EDX method was performed and the results are given in Table 2. Those data show that the composition of  $\beta$  phase corresponds to the chemical composition of the alloy, while the  $\alpha$  phase besides dominant titanium (>92 at.%) contained niobium and also chromium in a very small amount (<1 at.%). Hence,  $\beta$  phase is the solid solution of chromium and niobium in  $\beta$ -Ti, while the  $\alpha$  phase is the solid solution of niobium in  $\alpha$ -Ti with negligibly chromium content.

#### 3.2. Mechanical properties

The results of Vickers hardness measurement are listed in Table 3 and they are very similar to those for other biomedical titanium alloys with niobium addition. For example, Vickers hardness values of Ti–10Mo– $x$ Nb alloys ( $x = 3, 7, 10$ ) were between 394 and 441 HV [13], while those for alloys in Ti–Nb–Zr–X system (X = Cr, Fe, Ta) were between 400 and 500 HV [7]. The highest hardness was measured for alloy Ti<sub>80</sub>Cr<sub>10</sub>Nb<sub>10</sub> which has the finest distribution of  $\alpha$  phase in  $\beta$ -matrix (Fig. 1a). It follows that crucial effect among alloys with identical phase constitution ( $\alpha + \beta$ ) have the grain size of  $\alpha$  phase and the way of its distribution. Hardness of as-cast Ti–Cr–Nb alloys was higher when  $\alpha$ -grains crystallized in  $\beta$ -matrix were smaller. So, Ti<sub>70</sub>Cr<sub>10</sub>Nb<sub>20</sub> alloy with the largest  $\alpha$ -grains in the microstructure (Fig. 1b) exhibits the smallest hardness value.

Elastic moduli of investigated alloys were determined from stress–compression curves shown in Fig. 3. As can be seen, all alloys, except Ti<sub>80</sub>Cr<sub>10</sub>Nb<sub>10</sub>, exhibit an elastic deformation stage followed by a long plastic deformation stage and coexisting high strength and large plasticity. From the experiment calculated values of elastic modulus ( $E$ ), compressive strength ( $R_{\text{mc}}$ ), yield strength ( $YS$ ) and plastic strain ( $\varepsilon$ ) are shown in Table 3. Those data show relatively low elastic modulus (17–55 GPa) of as-cast Ti–Cr–Nb alloys depending on their chemical compositions accompanied by the identical phase constitution ( $\alpha + \beta$ ). The lowest  $E$ -values have alloys with high niobium (20 and 30 at.%) and small chromium (10 at.%) content. In accordance, the highest  $E$ -values have

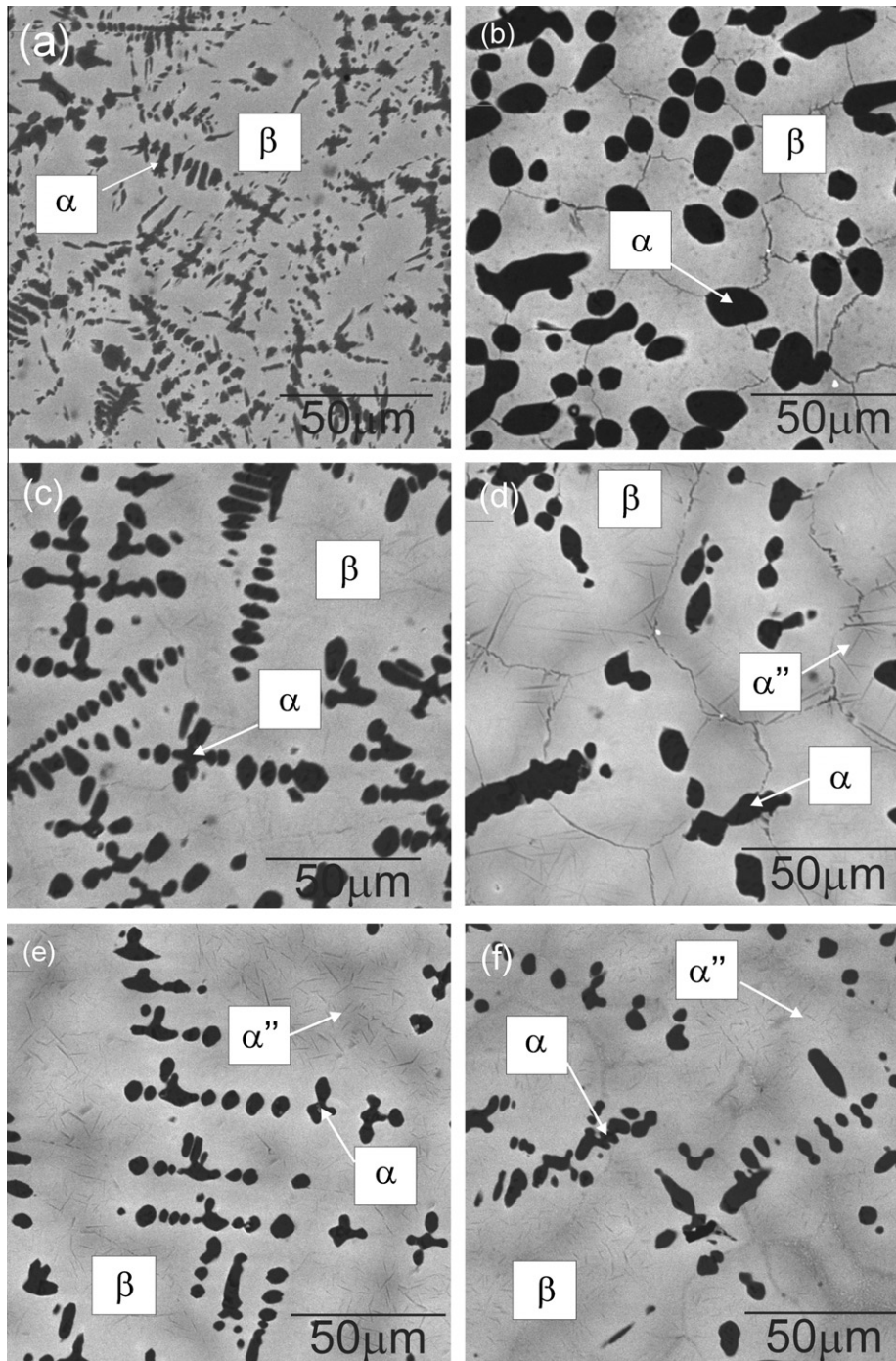


Fig. 1. SEM micrographs of as-cast Ti–Cr–Nb alloys.

alloys with the lowest niobium and the highest chromium content. Therefore elastic modulus of as-cast Ti–Cr–Nb alloys increases with chromium content and decreases with niobium which stabilizes  $\beta$ -phase with lower  $E$ -values than  $\alpha$ -phase [5]. These values exhibited considerably lower than  $E$ -values for other Ti–Cr alloys and Ti–Nb based alloys. For example, the minimum value for elastic modulus of binary Ti–Cr alloys in [19] was measured to be 100 GPa in Ti–5Cr alloy (wt.%), while in Ti–10Cr, Ti–20Cr and Ti–30Cr were 163 GPa, 128 GPa and 147 GPa respectively. Among ternary alloys Ti–5Cr– $x$ Fe [20], the minimum  $E$ -modulus value showed alloy Ti–5Cr–5Fe (76 GPa). The minimum value of  $E$ -modulus (50 GPa) among biomedical Ti–(18–28)Nb–(0.5–1.5)Si

alloys exhibited Ti–26Nb–1.0Si [6], while 24.7 GPa was measured in Ti–10Mo–10Nb alloy [13]. The yield strengths (690–1440 MPa) of investigated alloys were closely with those for the similar Ti–Nb based alloys, such as above mentioned alloy Ti–10Mo–10Nb (1404 MPa) [13]. Besides, all experimental alloys showed very high compressive strengths (825–2195 MPa), which are claimed for biomedical applications. The lowest yield strength values, as well as the compressive strengths, showed Ti<sub>80</sub>Cr<sub>10</sub>Nb<sub>10</sub> alloy with the highest titanium and the lowest chromium content. Contrary to this, the highest yield strength showed Ti<sub>60</sub>Cr<sub>30</sub>Nb<sub>10</sub> alloy with the minimal titanium and the maximal chromium content. In both cases niobium content was the same, i.e. 10 at.%. These alloys also

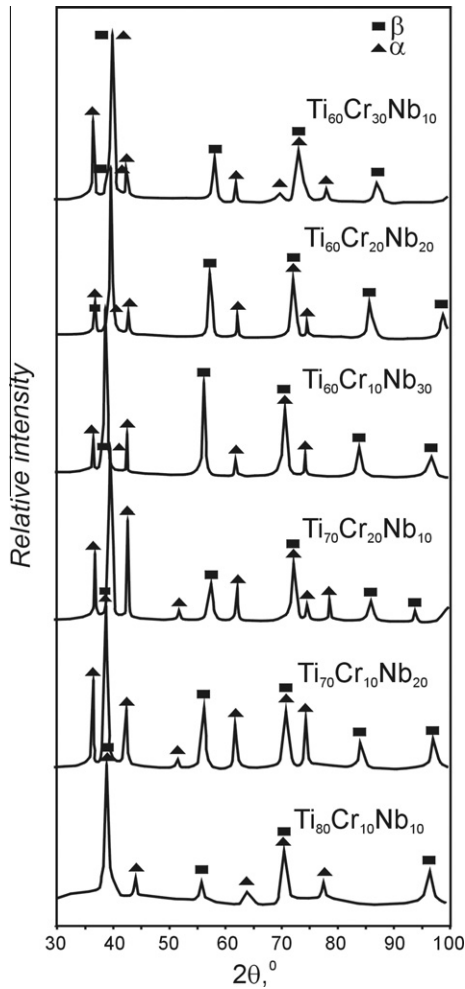


Fig. 2. XRD patterns of as-cast Ti–Cr–Nb alloys.

Table 1  
Chemical compositions of experimental alloys and lattice parameters of the constituent phases in as-cast Ti–Cr–Nb alloys.

Alloy composition (at.%)	β-phase		α-phase	
	a (nm)	c (nm)	a (nm)	c (nm)
Ti <sub>80</sub> Cr <sub>10</sub> Nb <sub>10</sub>	0.3254	0.2944	0.2944	0.4682
Ti <sub>70</sub> Cr <sub>10</sub> Nb <sub>20</sub>	0.3247	0.2942	0.2942	0.4659
Ti <sub>70</sub> Cr <sub>20</sub> Nb <sub>10</sub>	0.3197	0.2944	0.2944	0.4683
Ti <sub>60</sub> Cr <sub>10</sub> Nb <sub>30</sub>	0.3253	0.2941	0.2941	0.4622
Ti <sub>60</sub> Cr <sub>20</sub> Nb <sub>20</sub>	0.3204	0.2943	0.2943	0.4664
Ti <sub>60</sub> Cr <sub>30</sub> Nb <sub>10</sub>	0.3153	0.2945	0.2945	0.4671

Table 2  
EDX analysis results of as-cast Ti–Cr–Nb alloys (in at.%).

Alloy	Phase	Ti	Cr	Nb
Ti <sub>80</sub> Cr <sub>10</sub> Nb <sub>10</sub>	β	81.91	9.63	8.46
	α	95.98	0.87	3.15
Ti <sub>70</sub> Cr <sub>10</sub> Nb <sub>20</sub>	β	67.99	10.54	21.47
	α	93.74	0.36	5.90
Ti <sub>70</sub> Cr <sub>20</sub> Nb <sub>10</sub>	β	67.71	22.54	9.75
	α	96.67	0.70	2.63
Ti <sub>60</sub> Cr <sub>10</sub> Nb <sub>30</sub>	β	62.66	8.42	28.92
	α	92.05	0.29	7.66
Ti <sub>60</sub> Cr <sub>20</sub> Nb <sub>20</sub>	β	63.30	19.22	17.48
	α	95.24	0.58	4.18
Ti <sub>60</sub> Cr <sub>30</sub> Nb <sub>10</sub>	β	59.57	29.64	10.79
	α	96.69	0.75	2.56

Table 3  
Mechanical properties as-cast Ti–Cr–Nb alloys.

Alloy	HV2	E (GPa)	YS (MPa)	R <sub>mc</sub> (MPa)	ε (%)
Ti <sub>80</sub> Cr <sub>10</sub> Nb <sub>10</sub>	575	29	690	825	32.0
Ti <sub>70</sub> Cr <sub>10</sub> Nb <sub>20</sub>	412	17	1180	1580	75.0
Ti <sub>70</sub> Cr <sub>20</sub> Nb <sub>10</sub>	522	50	980	1590	83.5
Ti <sub>60</sub> Cr <sub>10</sub> Nb <sub>30</sub>	525	19	1100	2195	40.5
Ti <sub>60</sub> Cr <sub>20</sub> Nb <sub>20</sub>	484	28	1015	1700	78.5
Ti <sub>60</sub> Cr <sub>30</sub> Nb <sub>10</sub>	504	55	1440	2050	70.5

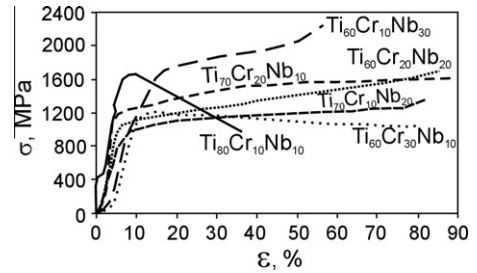


Fig. 3. Room-temperature compressive stress–strain curves of Ti–Cr–Nb alloys.

exhibited excellent plasticity (32.0–83.5%), which is a significantly higher than that for similar biomedical alloys with niobium addition, such as Ti–10Mo–10Nb (30.81%) [13].

### 3.3. Corrosion resistance

The corrosion resistance of as-cast Ti–Cr–Nb alloys was evaluated by the potentiodynamic polarization technique on the basis of  $E_{pitt}$  values. The anodic polarization curves for experimental alloys are presented in Fig. 4. Corrosion potentials ( $E_{corr}$ ) were approximately –500 mV/SCE for all of the alloys, which is in a good agreement with other published results. For alloy Ti–30Nb–15Zr corrosion potential was measured to be –596 mV [21] and for Ti–8Ta–3Nb measured values were 370–490 mV [22]. At potentials above  $E_{corr}$ , small significant differences in current densities were observed among tested alloys. The passive current densities were much lower for alloys with higher niobium content due to the formation of very stable niobium oxide layer ( $Nb_2O_5$ ) on the metal surface [23]. Pitting corrosion was stimulated by polarizing the specimen to noble potentials until the oxide layer breakdowns. This passive layer mainly consisting of  $TiO_2$  and  $Nb_2O_5$ , which forms naturally and protects the underlying, highly reactive titanium metal against uncontrolled chemical or biochemical reactions and corrosion [22]. In Table 4 are listed measured breakdown potentials ( $E_{pitt}$ ) for experimental alloys. Those high

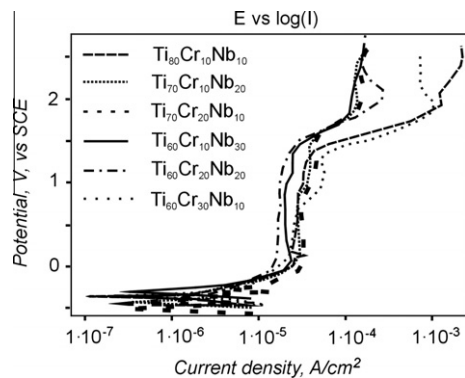


Fig. 4. Anodic polarization curves of Ti–Cr–Nb alloys.

**Table 4**  
Electrode potentially (vs SCE) of as-cast Ti–Cr–Nb alloys.

Alloy	$E_{\text{pitt}}$ (mV)
Ti <sub>80</sub> Cr <sub>10</sub> Nb <sub>10</sub>	1350
Ti <sub>70</sub> Cr <sub>10</sub> Nb <sub>20</sub>	1510
Ti <sub>70</sub> Cr <sub>20</sub> Nb <sub>10</sub>	1495
Ti <sub>60</sub> Cr <sub>10</sub> Nb <sub>30</sub>	1420
Ti <sub>60</sub> Cr <sub>20</sub> Nb <sub>20</sub>	1340
Ti <sub>60</sub> Cr <sub>30</sub> Nb <sub>10</sub>	1320

data (1320–1510 mV) reveal a very good stability of the passive oxide film that forms spontaneously on the surface of metal, indicating excellent biocompatibility of investigated Ti–Cr–Nb alloys.

#### 4. Conclusions

This study was conducted to develop titanium-based alloys with new chemical compositions and adequate microstructure and properties for biomedical applications. From the presented results it can be concluded as follows:

- Microstructural observation performed by SEM with BSE technique showed that all alloys consist of two phases. However, in alloys with 60 at.% of Ti the third needle-like  $\alpha''$  phase was observed too.
- XRD analysis revealed that all of six as-cast Ti–Cr–Nb alloys consist of  $\beta$  and  $\alpha$  phase, while the  $\alpha''$  phase was not detected probably due to its small amount.
- EDX method revealed that the  $\beta$  phase is solid solution of chromium and niobium in  $\beta$ -Ti, while the  $\alpha$  phase is the solid solution of niobium in  $\alpha$ -Ti with venial chromium content.
- Lattice parameter of  $\beta$  and  $\alpha$  phases were reduced by comparison with those for pure  $\beta$ - and  $\alpha$ -Ti, through the formation of the  $\beta$ - and  $\alpha$ -Ti solid solutions, since the atomic radius of substitutional alloying elements (chromium and niobium) were smaller than that for titanium.
- Major effects on Vickers hardness of investigated alloys have the grain size of  $\alpha$  phase and the way of its distribution. Therefore, hardness increases when the size of the  $\alpha$ -grains crystallized in  $\beta$ -matrix decreases.
- The low values of elastic modulus obtained for experimental alloys were the result of niobium addition, as an element which stabilizes the  $\beta$  phase with lower  $E$ -modulus than the  $\alpha$  phase. Nearly all alloys exhibit high strength and large plasticity.
- Very similar and high pitting potential values indicated a very good stability of the passive oxide film, i.e. the corrosion resistance of alloys, which was not significantly affected by their chemical compositions.

According to the presented results it could be considered that new biomedical alloys were developed. Namely, Ti<sub>70</sub>Cr<sub>10</sub>Nb<sub>20</sub>,

Ti<sub>70</sub>Cr<sub>20</sub>Nb<sub>10</sub> and Ti<sub>60</sub>Cr<sub>20</sub>Nb<sub>20</sub> alloys have the properties required for use in a biomedicine, i.e. the low elastic modulus, high strength and plasticity, as well as the excellent corrosion stability.

#### Acknowledgment

This work was financially supported by the Ministry of Science, Education and Sports of the Republic of Croatia.

#### References

- [1] Zhou YL, Niinomi M, Akahori T. Effects of Ta content on Young's modulus and tensile properties of binary Ti–Ta alloys for biomedical applications. *Mater Sci Eng A* 2004;371:283–90.
- [2] Majumdar P, Singh SB, Chakraborty M. Elastic modulus of biomedical titanium alloys by nano-indentation and ultrasonic techniques – a comparative study. *Mater Sci Eng A* 2008;489:419–25.
- [3] Kim SE, Jeong HW, Hyun YT, Lee YT, Jung CH, Kim SK, et al. Elastic modulus in vitro biocompatibility of Ti–xNb and Ti–xTa alloys. *Met Mater Int* 2007;13:145–9.
- [4] Kim H-K, Jang J-W. Electrochemical corrosion behavior and MG-63 osteoblast-like cell response of surface-treated titanium. *Met Mater Int* 2004;10:439–46.
- [5] Niinomi M. Recent metallic materials for biomedical applications. *Met Mater Trans* 2002;33A:477–86.
- [6] Kim H-S, Kim W-Y, Lim S-H. Microstructure and elastic modulus of Ti–Nb–Si ternary alloys for biomedical applications. *Scripta Mater* 2006;54:887–91.
- [7] Niinomi M, Akahori T, Takeuchi T, Katsura S, Fukui H, Toda H. Mechanical properties and cyto-toxicity of new beta type titanium alloy with low melting points for dental applications. *Mater Sci Eng C* 2005;25:417–25.
- [8] ASM handbook vol. 3, Alloy phase diagrams. OH: ASM International; 2002.
- [9] Koike M, Itoh M, Okuno O, Kimura K, Takeda O, Okabe TH, et al. Evaluation of Ti–Cr–Cu alloys for dental applications. *J Mater Eng Perform* 2005;14:778–83.
- [10] Powder diffraction file search manual. CPDS International Centre for Diffraction Data, Newtown Square; 2006.
- [11] [http://www.ccp14.ac.uk/tutorial/lmgp/celref\\_manual\\_hkl\\_peaks.html](http://www.ccp14.ac.uk/tutorial/lmgp/celref_manual_hkl_peaks.html) [accessed 14.12.10].
- [12] He G, Hagiwara M. Ti alloy design strategy for biomedical applications. *Mater Sci Eng C* 2006;26:14–9.
- [13] Xu LJ, Chen YY, Liu ZG, Kong FT. The microstructure and properties of Ti–Mo–Nb alloys for biomedical applications. *J Alloys Compd* 2008;453:320–4.
- [14] Guo Q, Zhan Y, Mo H, Zhang G. Aging response of the Ti–Nb system biomaterials with  $\beta$ -stabilizing elements. *Mater Des* 2010;31:4842–6.
- [15] Taneichi K, Taira M, Sukekai E, Narushima T, Iguchi Y, Ouchi C. Alloy design and property evaluation of new  $\beta$  type titanium alloy with excellent cold workability and biocompatibility. *ISIJ Int* 2006;46:292–301.
- [16] Xiong J, Li Y, Wang X, Hodgson P, Wen C. Mechanical properties and bioactive surface modification via alkali-heat treatment of a porous Ti–18Nb–4Sn alloy for biomedical applications. *Acta Biomater* 2008;4:1963–8.
- [17] Mantani Y, Tajima M. Phase transformation of quenched  $\alpha'$ -martensite by aging in Ti–Nb alloys. *Mater Sci Eng A* 2006;438–440:315–9.
- [18] Cui CY, Ping DH. Microstructural evaluation and ductility improvement of a Ti–30Nb alloy with Pd addition. *J Alloys Compd* 2009;471:248–52.
- [19] Ho WF, Chang TY, Wu SC, Hsu HC. Mechanical properties and deformation behavior of cast binary Ti–Cr alloys. *J Alloys Compd* 2009;468:533–8.
- [20] Ho WF, Pan CH, Wu SC, Hsu HC. Mechanical properties and deformation behavior of Ti–5Cr–xFe alloys. *J Alloys Compd* 2009;472:546–50.
- [21] Martins DQ, Osório WR, Souza MEP, Caram R, Garcia A. Effects of Zr content on microstructure and corrosion resistance of Ti–30Nb–Zr casting alloys for biomedical applications. *Electrochim Acta* 2008;53:2809–17.
- [22] Karayan AI, Park SW, Lee KM. Corrosion behavior of Ti–Ta–Nb alloys in simulated physiological media. *Mater Lett* 2008;62:1843–5.
- [23] Eisenbarth E, Velten D, Müller M, Thull R, Breme J. Biocompatibility of  $\beta$ -stabilizing elements of titanium alloys. *Biomaterials* 2004;25:5705–13.